Research article

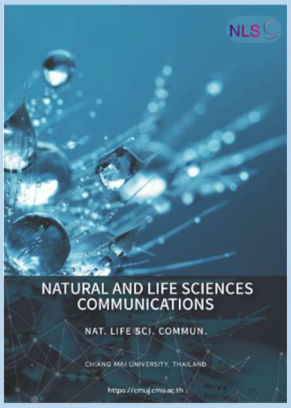

Editor:
Wipawadee Yooin,
Chiang Mai University, Thailand

Article history:
Received: June 20, 2023;
Revised: September 22, 2023;
Accepted: October 20, 2023;
Online First: October 30, 2023
https://doi.org/10.12982/NLSC.2023.070

Corresponding author:
Sureewan Duangjit,
E-mail: sureewan.d@ubu.ac.th

Comparative and Stability Study of Rice Bran Oil in Nanovesicle: Conventional Niosomes and pH-Sensitive Niosomes

Sureewan Duangjit[1,*], Chudanut Akarachinwanit[1], Warisada Sila-on[2], Sureewan Bumrungthai[1] Praneet Opanasopit[3] and Tanasait Ngawhirunpat[3]

1 Division of Pharmaceutical Chemistry and Technology, Faculty of Pharmaceutical Sciences, Ubon Ratchathani University, Ubon Ratchathani, 34190 Thailand.
2 Department Pharmaceutical Technology, College of Pharmacy, Rangsit University, Pathum Thani, 12000, Thailand.
3 Department of Pharmaceutical Technology, Faculty of Pharmacy, Silpakorn University, Nakhon Pathom 73000 Thailand.

ABSTRACT

Niosomes are more stable and economical than liposomes. In previous studies, conventional niosomes have shown advantages for transdermal delivery of bioactive compounds from rice bran. The objective of this study was to compare nanovesicle formulations (conventional niosomes and pH-sensitive niosomes) containing oryzanol (OZ) and rice bran oil (RBO). The formulation parameters were varied for the types of model drugs (OZ pure compound and RBO), the content of RBO loading (low, medium, high), and the types of niosomes (conventional niosomes and pH-sensitive niosomes). The physicochemical properties, e.g., vesicle size, size distribution, zeta potential and oryzanol content, were investigated. The stability of nanovesicles during the incubation period from Day 1 to Day 90 was observed. The *in vitro* skin permeation of the niosome formulation was demonstrated and calculated from the skin permeation flux and the permeability coefficient. The results indicated that the OZ- and RBO-loaded nanovesicle formulation had nanoscale vesicles (under 205 nm) and a narrow size distribution (0.22-0.55). The OZ content in the formulation was up to 300 µg/mL. The RBO-loaded nanovesicle formulations were stable at 4 and 25 °C for 90 days and 40 °C for 30 days. The skin permeation parameters of pH-sensitive niosomes were significantly higher than those of conventional niosomes at a flux of 16.56 ± 3.37 µg/cm^2/h and a permeability coefficient of 0.0542 ± 0.011 cm^2/h. These results suggest that pH-sensitive niosomes can be promoted and used as drug delivery carriers for rice bran oil.

Keywords: Floral biology, Flower, Pollen, Microclimate, Heat unit Rice bran, Oryzanol, Liposome, Oleic acid, Permeability coefficient

Funding: The authors are grateful for the research funding provided by the National Research Council of Thailand (NRCT): N42A650551 and the Office of the Higher Education Commission and the Thailand Research Fund (Grant no. RGNS 64−237).

Citation: Duangjit, S., Akarachinwanit, C., Sila-on, W., Bumrungthai, S., Opanasopit, P., and Ngawhirunpat, T. 2023. Comparative and stability study of rice bran oil in nanovesicle: Conventional niosomes and pH-sensitive niosomes. Natural and Life Sciences Communications. 22(4): e2023070.

INTRODUCTION

Rice bran oil (RBO) is a bioactive phytochemical source of nutraceuticals such as vitamin B (thiamine, riboflavin, niacin), vitamin E (tocopherol), folic acid, essential oils and minerals (magnesium, manganese, and zinc) and dietary fibers. Oryzanol (OZ) also occurs as a component of RBO, and four major bioactive compounds are found, e.g., cycloartenyl ferulate, 24-methylenecycloartanyl ferulate, campesteryl ferulate, and sitosteryl ferulate.(Cho et al., 2012) Several nanovesicles incorporating OZ or RBO have been considered successful carriers in delivery systems, such as microemulsions (Wuttikul and Boonme, 2016), nanoemulsions (Bernardi et al., 2011), solid lipid nanoparticles (SLNs) (Seetapan et al., 2010), nanostructured lipid carriers (NLCs) (Villar, Vidallon, and Rodriguez, 2022), liposomes (Viriyaroj et al., 2009), and niosomes (Manosroi et al., 2012a, 2012b).

Niosomes are nonionic surfactant-based nanovesicles with self-assembled closed bilayer structures. Niosomes are able to entrap both hydrophilic and lipophilic compounds similar to liposomes. Previously, niosome studies have shown advantages for the topical and transdermal delivery of various drug substances. Furthermore, niosomes are more beneficial characteristics of greater stability, smaller particle sizes, and lower cost than liposomes, ethosomes and transfersomes (Manosroi et al., 2008; Manosroi et al., 2012a, 2012b).

The intrinsic properties of the model drug and surfactant used, the cholesterol ratio used and the critical packing parameter (CPP) were the factors affecting the structure of niosomes. Thus, niosomes can be designed and developed for use in several drug delivery systems (Khoee and Yaghoobian, 2017). Our previous study focused on investigating the method of preparation using a probe and bath type sonicator (Akarachinwanit et al., 2017). However, studies on the individual contents of pure OZ compounds and OZ in RBO have not yet been conducted. In this study, we attempt to introduce a new niosome formulation for RBO delivery carriers. The objective of this study was to compare nanovesicle formulations (conventional niosomes and pH-sensitive niosomes) containing oryzanol (OZ) and rice bran oil (RBO). The formulation parameters were varied for the types of model drugs (OZ pure compound and RBO), the content of RBO loading (low, medium, high), and the types of niosomes (conventional niosomes and pH-sensitive niosomes). The physicochemical properties, e.g., vesicle size, size distribution, zeta potential and oryzanol content, were investigated. The stability of nanovesicles during the incubation period from Day 1 to Day 90 was observed. Moreover, the in vitro skin permeation of the niosome formulation was demonstrated using Franz diffusion cells. The permeability coefficient (Kp) was calculated from the skin permeation flux and the initial concentration of OZ in the donor compartment.

MATERIALS AND METHODS

Materials

All rice bran oil (RBO) was obtained from the Agricultural Cooperative Ltd. Ubon Ratchathani Province. RBO has an oryzanol content of 10 g/L. Oryzanol (OZ) was supplied by Tokyo Chemical Industry Co., Ltd. (Tokyo, Japan). Oleic acid was supplied by Sigma–Aldrich (Buchs, Switzerland). Tween 60 (T60) and cholesterol (Chol) were purchased from FUJIFILM Wako Pure Chemical Corporation (Osaka, Japan). All other chemicals used were of reagent grade and were purchased from Chemical Express Co., Ltd. (Bangkok, Thailand).

Preparation of niosomes and pH-sensitive niosomes

In this study, the formulation parameters were varied for the types of model drugs (OZ pure compound and RBO), the content of RBO loading (low (L), medium (M), high (H)) and the types of niosomes (conventional niosomes (NS) and pH-sensitive niosomes (pH-NS)). OZ- and RBO-loaded nanovesicles were prepared using the thin film hydration method. The formulations contained a constant amount of nonionic surfactant (Tween® 60; T60) and cholesterol (Chol) (1:1). Oleic acid (OA), as a penetration enhancer and a pH-sensitive molecule, was also varied, as shown in Table 1. The OZ in the RBO ranged from 0.3, 0.6 and 1.2 g/L for low, medium and high RBO loadings, respectively. The lipid mixture was dissolved in chloroform: methanol (2:1 v/v) and evaporated by using a nitrogen stream. The dried lipid film was hydrated with a phosphate buffer solution (PBS; pH 7.4). All formulations were subsequently sonicated using a probe-type sonicator (Vibra-Cell™; Sonics and Materials, Inc., Newtown, CT, USA) for 2 cycles of 15 min. The temperature during the process of sonication was controlled at 50 °C (Xu et al., 2016). The excess OZ and lipids in the formulation were removed by centrifugation at 14,000 rpm for 15 min. The nanovesicles were freshly prepared and stored in airtight containers at 4 °C prior to use.

Physicochemical characterization

The average vesicle size, size distribution and zeta potential of the OZ-loaded nanovesicles were determined by photon correlation spectroscopy (PCS) (Zetasizer Nano series, Malvern Instruments, UK). All measurements were taken at room temperature (25 °C). Twenty microliters of the nanoscale vesicles were diluted with 1480 µL of deionized water. At least three independent measurements were recorded.

The OZ concentration in the formulation of all samples was determined after vesicle disruption with 0.1% Triton® X-100 at a 1:1 volume ratio and appropriate dilution with phosphate buffer solution (pH 7.4). The nanoscale vesicle/Triton® X-100 solution was centrifuged at 10,000 rpm at 25 °C for 10 min. The supernatant was filtered through a 0.45 µm nylon syringe filter and then analyzed by HPLC.

Table 1. The composition of nanovesicle formulations.

Formulation	Composition (g)				
	T60	Chol	OA	RBO	PBS pH 7.4
F1: NS	9.2	2.7	-	-	1000 mL
F2: pH-NS	9.2	2.7	0.6	-	1000 mL
F3: NS-RBO	9.2	2.7	-	0.3 (L) 0.6 (M) 1.2 (H)	1000 mL
F4: pH-NS-RBO	9.2	2.7	0.6	0.3 (L) 0.6 (M) 1.2 (H)	1000 mL
F5: pH-NS-OZ	9.2	2.7	0.6	0.6 (OZ)	1000 mL

Note: Abbreviation: Niosomes; NS, pH-sensitive noisome; pH-NS, Tween® 60; T60, cholesterol; Chol, oleic acid; OA, rice bran oil; RBO, oryzanol powder; OZ, phosphate buffer saline pH 7.4; PBS pH 7.4, low amount of RBO; L, medium amount of oil; M, high amount of oil; H

HPLC analysis

The concentration of OZ in all formulations was analyzed using HPLC (Thermo Scientific™ UltiMate 3000 UHPLC System). A C18 reversed-phase column (Symmetry®, VertiSep™, Vertical, Thailand) with dimensions of 5 µm and 4.6×150 mm was utilized. A mixture of methanol, acetonitrile and 1% acetic acid (52:45:3) was used as the mobile phase for gamma-oryzanol determination (Yoshie et al., 2009). The detector was UV at 330 nm with a flow rate of 1.0 ml/min and an injection volume of 20 µL. The retention time was 45 min. The calibration curves for OZ were in the range of 1-100 µg/ml with a correlation coefficient of 0.99.

Stability study

The stability of the nanovesicles was investigated by monitoring the formulations for at least 90 days after the initial formulation. The nanovesicles were kept in glass bottles with plastic plugs at 4 ± 1, 25 ± 1 and 40 ± 1 °C to determine the stability of the formulations. The physicochemical stabilities of the nanovesicle formulations were evaluated for sedimentation and phase separation by visual inspection. The vesicle size, size distribution and zeta potential were measured by PCS.

In vitro skin permeation

To compare the permeation of RBO in nanovesicle formulations, *in vitro* skin permeation was performed through the shed snake skin using Franz-type cells (n=3) at 37 °C. Wonglertnirant et al. used the shed snake skin of *Naja kaouthia* as a model for skin permeation due to its similarity to the stratum corneum of humans (Wonglertnirant, Ngawhirunpat, and Kumpugdee-Vollrath, 2012). Shed snake skin obtained from the Queen Saovabha Memorial Institute, Thai Red Cross Society, Bangkok, Thailand, was used as a skin model for this study. The shed snake skin was obtained immediately after shedding and stored at -20 °C prior to use. The estimated skin thickness was 0.02–0.03 mm. The same shed snake skin was cut into 10 to 12 pieces of 2.5 cm x 2.5 cm round sections. The shed snake skin was thawed and immediately placed on a Franz diffusion cell. A Franz diffusion cell with an available permeation area of 2.01 cm^2 and a water jacket at 37 ± 1 °C was employed. The stratum corneum side of the shed snake skin faced the donor chamber, and 1 mL of nanovesicle formulations was filled. The receiving chamber was filled with 12.5 mL of receiver medium (PBS pH 7.4:EtOH; 1:1 v/v) under sink conditions and stirred by a magnetic stirrer at 150 rpm. At appropriate intervals, 0.5 mL aliquots of the receiver medium were withdrawn and immediately replaced with an equal volume of fresh buffer. The OZ in the receiver medium was analyzed by HPLC. The cumulative amount of OZ that permeated through the skin was plotted as a function of time. The steady-state flux (J) was defined after calculating the slope of the linear portion of the plot. The permeability coefficient (Kp) was determined by the following equation:

$$Kp = J_{ss}/C_0$$

where C_0 is the OZ initial concentration in the donor compartment. Stationary drug flux (J_{ss}, µg/cm^2/h) was calculated from the relation between the slope of the plot of the quantity of permeated drug vs. time and the area exposed (2.01 cm^2) (Khurana, Jain, and Bedi, 2013; Peralta et al., 2018).

Data analysis

The data are reported as the mean ± standard deviation (SD) (n=3). A *P* value of less than 0.05 was considered to be significant. The statistical analysis of the data was performed with IBM® SPSS® Statistics (version 26, IBM, New York, USA) using one-way ANOVA followed by Tukey's test.

RESULTS

Physicochemical characterization

The physicochemical properties of the OZ- and RBO-loaded nanovesicle formulations are shown in Figure 1. The formulation factors, e.g., (i) types of model drugs (OZ and RBO), (ii) content of RBO loading (low, medium, high), and (iii) types of niosomes (conventional niosomes and pH-sensitive niosomes), were compared. Phase separation was observed in the RBO-H-loaded nanovesicles in both conventional niosomes and pH-sensitive niosomes. The mixture of RBO-H overloading and nanovesicles was separated before analysis. The physicochemical stability of the remaining RBO-H-loaded nanovesicles was also investigated because the vesicle size, size distribution, zeta potential and OZ content can be determined in the aqueous phase of nanovesicles. However, the yield of RBO-H-loaded nanovesicles was significantly lower than that of RBO-L- and RBO-M-loaded nanovesicles. and August) at Ban Phaeo District, Samut Sakhon Province, Thailand in 2020.

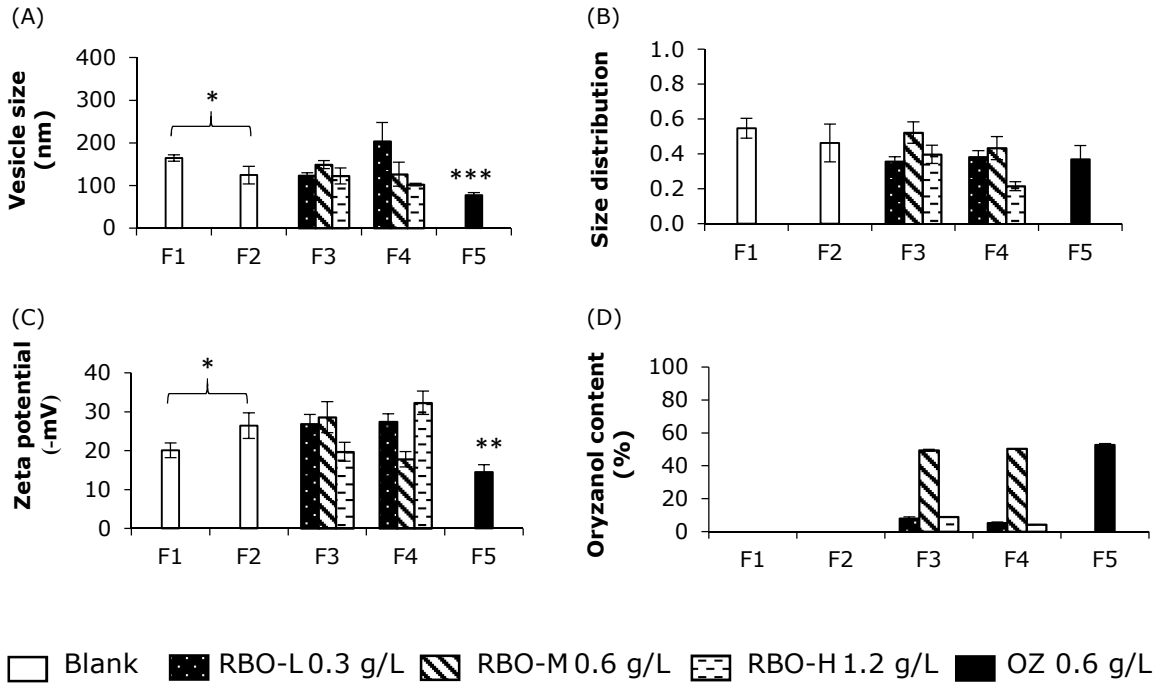

Figure 1. The physicochemical properties of nanovesicle formulation: vesicle size (A), size distribution (B), zeta potential (C) and oryzanol (OZ) content(D) in the formulation. * significance, ** significantly compared with F2, *** significantly compared with other formulations.

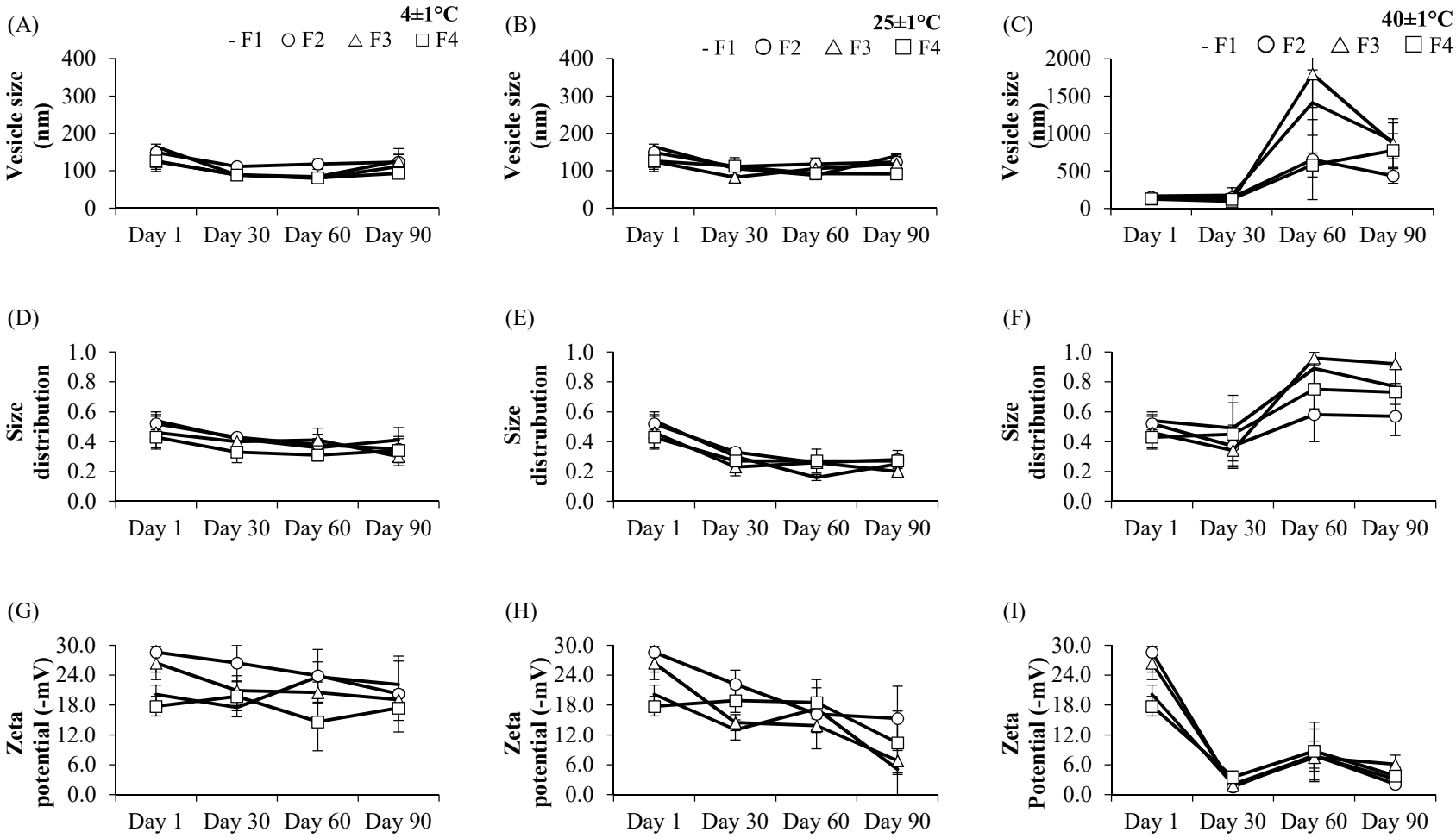

Figure 2. The physicochemical properties of nanovesicle formulation at 4, 25 and 40°C: (A-C) vesicle size, (D-F) size distribution and (G-I) zeta potential.

The vesicle size of blank nanovesicles (F1, F2), RBO-loaded nanovesicles (F3, F4) and OZ-loaded pH-sensitive niosomes (F5) was smaller than 205 nm, with a size distribution between 0.22 and 0.55 (Figure 1A and Figure 1B). The zeta potential of all formulations was negative, between 14-32 (-mV) (Figure 1C). The OZ content was 4-52% (Figure 1D). The formulation factors have an effect on the vesicle size, size distribution and zeta potential.

Stability study

The physicochemical stability of the nanovesicles is displayed in Figure 2. At the initial preparation (Day 1), phase separation was observed in the RBO-H-loaded nanovesicles in both conventional niosomes and pH-sensitive niosomes. The sedimentation of the colloidal system was observed in conventional niosomes (F1 and F3) at Days 60 and 90 under incubation conditions of 40 ± 1 °C. The physical appearance of the pH-sensitive niosomes (F2 and F4) was a white and clear solution. The conventional noisome and pH-sensitive niosomes were stable at 4 and 25 °C for 90 days.

***In vitro* skin permeation**

The concentration of OZ in RBO-M-loaded nanovesicle formulations was up to 300 µg/mL. The cumulative skin permeation per area of the pH-sensitive niosomes increased linearly after 2 h. The skin permeation flux of RBO was defined as the slope of the linear portion of the plot. Following the skin permeation profile, the results indicated that the cumulative skin permeation at 8 h of pH-sensitive niosomes was higher than that of the conventional niosomes and control (RBO in 50% ethanolic solution) (Figure 3). The skin permeation flux and the permeability coefficient (K_p) of conventional niosomes and pH-sensitive niosomes are shown in Table 2.

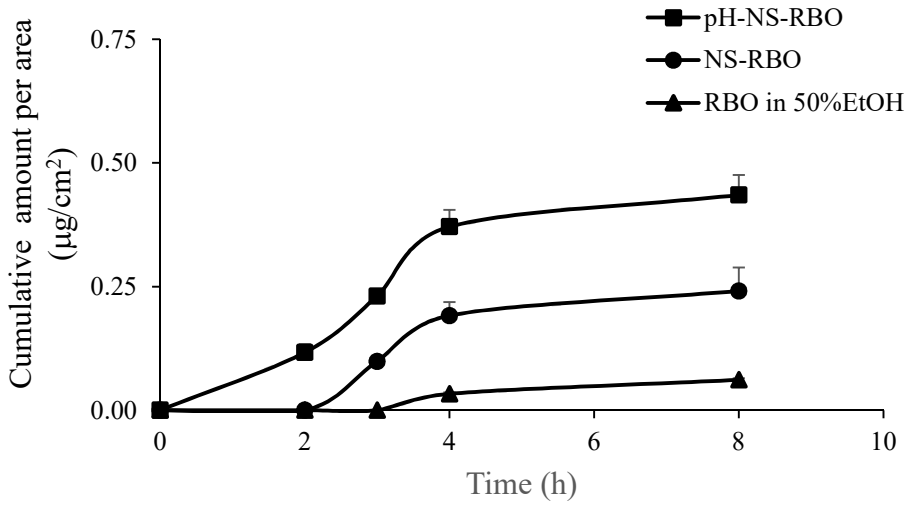

Figure 3. The skin permeation profile of oryzanol formulation

Table 2. The skin permeation parameter of oryzanol loaded nanovesicles

Formulation	Flux (µg/cm²/h)	C_0 (µg/mL)	K_p (cm²/h)
NS-RBO	10.57 ± 1.56 [a]	298.97 ± 10.78	0.0353 ± 0.005
pH-NS-RBO	16.56 ± 3.37 [b]	305.71 ± 10.58	0.0542 ± 0.011

Note: a the flux calculated from 2 – 4 h, b the flux calculated from 0 - 4 h

DISCUSSION

Physicochemical characterization

The incorporation of oleic acid and model drugs (both OZ and RBO) affects the vesicle size increase and decrease. Oleic acid is a monounsaturated fatty acid that is used as a solubilizer, penetration enhancer and pH-sensitive molecule in pH-sensitive liposomes. The vesicle size of blank pH-sensitive niosomes (F2) was significantly smaller than that of blank conventional niosomes (F1). The vesicle sizes of RBO-M- and RBO-H-loaded pH-sensitive niosomes (F4) were also significantly smaller than those of RBO-M- and RBO-H-loaded conventional niosomes (F3) (Figure 1A). Leekumjorm et al. suggested that the presence of unsaturated fatty acids reduced the packing between phospholipids, while saturated fatty acids increased the packing between phospholipids. (Leekumjorn et al., 2009) In contrast, the effect of oleic acid on vesicle size was consistent with that of nanoscale vesicles (liposomes and niosomes) incorporating methotrexate (Srisuk et al., 2012), caffeine (Abd, Roberts, and Grice, 2016), ellagic acid (Duangjit et al., 2016), zolmitriptan (Abd-Elal et al., 2016), and garlic extract (Pinilla, Thys, and Brandelli, 2019). These results may be due to the role of unsaturated fatty acids (oleic acid) in minimizing biophysical changes in the bilayer surface area (Leekumjorn et al., 2009).

OZ, a major constituent in RBO as a potential antioxidant, was incorporated into the nanovesicles. The incorporation of OZ led to a smaller vesicle size in OZ-loaded pH-sensitive niosomes (F5) compared to blank pH-sensitive niosomes (F2). Viriyaroj et al. suggested that the insertion of OZ, a hydrophobic molecule, results in the disintegration of the formation of transient structures in vesicles. Thus, the vesicle size of OZ-loaded vesicles was smaller than that of blank vesicles. (Viriyaroj et al., 2009) However, no remarkable decrease in vesicle size was observed in RBO-M-loaded nanovesicles (F3, F4) compared to blank nanovesicles of F1 and F2, respectively. The vesicle size of RBO-M-loaded nanovesicles (F3, F4) was significantly greater than that of OZ-loaded pH-sensitive niosomes (F5). The RBO-loaded nanovesicles were smaller than those of blank niosomes in a previous study. (Manosroi et al., 2012a) This may be related to the effect of bioactive components that are a rich source of phytochemicals, such as ferulic acid, oryzanol and phytic acid, which can be varied from the source of RBO.

The effect of the RBO-loaded nanovesicles was observed. The content of OZ was varied as 0.3, 0.6 and 1.2 g/L. The results indicated that an increase in OZ content led to a decrease in vesicle size in F4 (RBO-L > RBO-M > RBO-H). The vesicle size increased and decreased in F3. These results are in accordance with a previous report that an increase in OZ content led to an increase and decrease in the vesicle size of liposomes. There was no significant difference in vesicle size between niosomes incorporated with RBO-L and RBO-M or RBO-M and RBO-H. Whereas niosomes included RBO-L and RBO-H, the comparison was significant. The results indicated that both the amount of RBO and the method of preparation influence vesicle size. It is hypothesized that this phenomenon may be attributed to the effect of the preparation method. OZ-loaded liposomes incorporating different surfactants (sodium taurocholate and 3-cholamidopropyl dimethylammonio 1-propanesulfonate) exhibited different vesicle sizes (Viriyaroj et al., 2009) The different lipid compositions and oleic acid contents in F3 and F4 can cause different phenomena.

The effect of oleic acid on the vesicle size of blank pH-sensitive niosomes (F2), RBO-loaded pH-sensitive niosomes (F4) and OZ-loaded pH-sensitive niosomes (F5) was compared to that of conventional niosomes (F1 and F3). The addition of the pH-sensitive molecule oleic acid can promote the conversion

of plain niosomes to pH-sensitive niosomes. (Fan et al., 2017; Mertins, Mathews, and Angelova, 2020) The insertion of oleic acid, a fatty acid penetration enhancer, resulted in a decrease in vesicle size in this study. Although the lipid compositions affect the size of vesicles, the method of preparation also affected the vesicle size. (Akbarzadeh et al., 2013) These results indicated that the thin film hydration method in this study could produce small vesicles as active-loaded nanovesicles. Consequently, sonication was perhaps the most extensively used method for the preparation. (Abdelkader, Alani, and Alany, 2014; Chen et al., 2019; Khan et al., 2020; Mutlu-Agardan et al., 2021)

The size distribution was used as an indicator of nanoscale vesicle stability and uniformity. Vesicles with a wider range of vesicle sizes have a high polydispersity index (PDI), while monodisperse vesicles have a lower PDI. (Masarudin et al., 2015) The size distribution of all niosomes was between 0.22-0.55 with a slightly broad distribution but was still in the nanoscale range. The sonication time can vary from 15 to 30 min to minimize the size distribution variation. (Viriyaroj et al., 2009) The insertion of oleic acid, a fatty acid penetration enhancer, resulted in a decrease in the size distribution in this study. With the incorporation of RBO, no significant difference in size distribution was observed (Figure 1B). In addition to the lipid compositions, the method of preparation also affected the PDI. The narrow size distribution of niosomes prepared using the sonication method can be improved by improving the sonication time. A size distribution of 0.15 demonstrated a highly stable and retained homogeneous dispersion (Masarudin et al., 2015). The size distribution of 0.3 and below was acceptable and suggested as a homogenous formulation (Danaei et al., 2018). A size distribution over 0.7 indicated that the vesicles had a very broad size distribution.

The zeta potential is an intrinsic physicochemical property of nanovesicles that is directly influenced by the formulation factor. Tween 60 and cholesterol are nonionic molecules. The primary lipid compositions have no charge in their molecules; thus, the zeta potential should be zero. The results indicated that a negative zeta potential between 14-32 (-mV) was detected (Figure 1C). The blank conventional niosomes (F1) exhibited negative values of the zeta potential, which might be attributed to the adsorption of counter ions or the preferential adsorption of hydroxyl ions at the vesicle surface (Junyaprasert, Teeranachaideekul, and Supaperm, 2008). Based on the formulation factor of blank conventional niosomes (F1) and blank pH-sensitive niosomes (F2), oleic acid may be a key factor that affects the zeta potential of nanovesicles. Thus, the zeta potentials of conventional niosomes (F1 and F3) and pH-sensitive niosomes (F2 and F4) were also different. The incorporation of oleic acid and bioactive compounds (both OZ and RBO) dramatically affected the zeta potential. In comparison, the zeta potential of blank conventional niosomes (F1) was significantly smaller than that of blank pH-sensitive niosomes (F2); since the incorporation of a fatty acid (OA) at the environmental pH of 7.4, OA may partially dissociate (deprotonate) due to its pKa of 4.9 under this condition (Kurniawan, Suga, and Kuhl, 2017). Thus, F2 had a more negative charge than F1. Similarly, RBO is a source of ferulic acid (pKa 3.7), oryzanol (pKa 9.8) and phytic acid (pKa 5.2), which may influence the net zeta potential at the surface of niosomes. The zeta potentials of blank conventional niosomes (F1) and RBO-loaded niosomes (F3) were significantly different, except for RBO-H-loaded niosomes. The zeta potentials of blank pH-sensitive niosomes (F2) and RBO-loaded pH-sensitive niosomes (F4) were significantly different, except for RBO-L-loaded pH-sensitive niosomes. The effect of OZ in pH-sensitive niosomes (F5) resulted in a decrease in the zeta potential when compared to the blank pH-sensitive niosomes (F2). A decrease in zeta potential was also observed in a previous study with increasing OZ (Rodsuwan et al., 2020).

The OZ content in the formulation of RBO- and OZ-loaded nanovesicles is shown in Figure 1D. The content of OZ in RBO was varied as 0.3, 0.6 and 1.2 g/L. Although phase separation was obvious in the RBO-H-loaded nanovesicles, the OZ content was also detected in the aqueous phase of the formulation. The lower part was RBO-H loaded (aqueous phase), while the upper part of the separation was an excess RBO. Therefore, the OZ content declined with RBO-H compared to RBO-M. The amount of OZ in RBO-L and RBO-M can be incorporated into nanovesicle formulations. However, the addition of RBO-H to the nanovesicles was unsuccessful in this study. Previously, 0.2 to 0.5% date seed oil was added to niosomes with 2% Span 60 (Soliman et al., 2018). The essential oil of 0.5 to 2% can be incorporated in the niosomes with 6% Span 60 (Eid, Essa, and El Maghraby, 2019). This result indicated that the concentrated RBO with OZ should be considered in further studies. The loading capacity of RBO in the nanovesicles with 0.92% Tween 60 was not more than 0.6 g/L or 6% in this study. It could be considered that the different compositions of nanovesicles may affect the loading capacity of the niosome formulations.

Stability study

The vesicle size and size distribution of all formulations at Days 30, 60 and 90 at 4 ± 1 and 25 ± 1 °C were not significantly different from those on Day 1 (Figure 2A-2B and Figure 2D-2E). However, at 40 ± 1 °C, the vesicle size and size distribution of all formulations were obviously different from the initial day at Days 60 and 90 due to the sedimentation of the colloidal system (Figure 2C and 2F). The results indicated that the physiochemical stability (vesicle size and size distribution) of the pH-sensitive niosomes was more stable than that of the conventional niosomes. The presence of oleic acid in the pH-sensitive nanovesicles provided greater stability compared with conventional nanovesicles developed in a previous study (Pinilla, Thys, and Brandelli, 2019).

In comparison, the zeta potential of all formulations at 4 ± 1 and 25 ± 1 °C was slightly decreased at Days 30, 60 and 90 (Figure 2G and 2H). At 40 ± 1 °C, the zeta potential of all formulations dramatically decreased at Days 30, 60 and 90 compared to the initial value on Day 1 (Figure 2I). The decrease in zeta potential may result in an increase in vesicle size and vesicle aggregation because the attractive intervesicular forces predominate over the repulsive intervesicular forces (Guo, Heinämäki, and Yliruusi, 2008; Rodsuwan et al., 2020). The intrinsic study about the temperature effects on the zeta potential by Venditti (2008) revealed that the zeta potential of some solutions is strongly dependent upon the temperature (Venditti, 2008). In our study, the zeta potential was reduced with increasing temperature, coinciding well with a previous study (Al Mahrouqi et al. 2016). However, at 40 ± 1 °C, the zeta potentials of F2 and F4 tended to decrease, similar to the zeta potentials of F1 and F3. These results suggested that the system was stable when the vesicle size fell at the nanoscale, with a narrow size distribution under 0.7, and the surface charge showed that the repulsive forces predominated over the attractive forces. The vesicle size of nanovesicles had more influence on the dispersion of the colloidal system during the incubation condition than the zeta potential. In the case of nonionic surfactants, steric stability can prevent the aggregation of nanoscale vesicles (Hoeller, Sperger, and Valenta, 2009; Vonarbourg et al., 2009).

***In vitro* skin permeation**

The skin permeation profile suggested that the dramatic synergistic permeability-enhancing effect of the two types of niosomes was greater than that of the control ethanolic solution (50% EtOH). This result revealed that

nanovesicles act synergistically to improve the skin permeation of OZ. The skin permeation parameters (flux and K_p) of pH-sensitive niosomes were significantly higher than those of conventional niosomes. Skin permeation in this study was influenced by the following factors: (I) the vesicle size of niosomes emerges as a paramount determinant of skin permeation, irrespective of the specific form of nanovesicles under consideration (Patzelt et al., 2017); (II) the zeta potential of niosomes is a factor that determines the skin permeation efficiency of nanovesicles, and high skin permeation can be improved by a highly negative charge (Gillet et al., 2011); and (III) the drug load in niosome formulations can vary depending on the oryzanol load in nanovesicles. The incorporation of oleic acid has the ability to deliver oryzanol through the skin in different amounts. (Yu et al., 2021) A smaller vesicle size was the most significant factor in the skin permeation enhancement of the pH-sensitive noisome formulation in this study. The oleic acid–based nanovesicles provided good skin permeation of various drugs, such as fluconazole (Zakir et al., 2010), methotrexate (Srisuk et al., 2012), ellagic acid (Duangjit et al., 2016), and rosmarinic acid (Subongkot et al., 2021). In addition to oleic acid, cholesteryl hemisuccinate (Tokudome et al., 2025; Rinaldi et al., 2022) was used as a pH-sensitive agent in several studies. Oleic acid can improve skin penetration by increasing the lipid fluidity of the stratum corneum and intercellular lipids (Subongkot et al., 2021) and decreasing the order of the lipid membrane through intercalation between lipid bilayers. This effect is intensified by the cis isomer of the oleic acid hydrocarbon residue (Notman, Noro and Anwar, 2007).

The pH-sensitive niosome formulation may promote skin permeability via two mechanisms. The possible mechanisms by which this (i) pH-sensitive niosome formulation (as elastic vesicles) improved the skin permeation of OZ encompassed the penetration-enhancing mechanism and (ii) vesicle adsorption to and/or fusion with the stratum corneum (El Maghraby, Barry, and Williams, 2008). The pH-sensitive nanovesicle may be destabilized when the external pH is altered (Chu and Szoka, 1994), generally from neutral (pH 7.4) or slightly alkaline to acidic skin pH (pH 4 to 5.5) (Lambers et al., 2006). Abri Aghdam et al. (2019) reviewed the purpose of pH-sensitive nanovesicles in which the drug molecule can be released into the medium through fusion or destabilization of target membranes in the acidic conditions of the target tissue. The extravesicular pH of the medium is 7.4; thus, OZ may be released at an acidic pH of the skin site (Abri Aghdam et al., 2019). The possible mechanism underlying the effect of the OZ-loaded nanovesicle formulation on skin permeation enhancement should be confirmed by FTIR and DSC in further studies.

CONCLUSION

In the present study, novel pH-sensitive niosomes consisting of oleic acid as a penetration enhancer and a pH-sensitive molecule were successfully developed. The characterization showed that the types of model drugs (OZ pure compound and RBO), the content of RBO loading (low, medium, high), and the types of niosomes (conventional niosomes and pH-sensitive niosomes) affected the physicochemical characteristics and in vitro skin permeation. The skin permeation flux and the permeability coefficient of the RBO-M-loaded pH-sensitive niosomes were significantly higher than those of the RBO-M-loaded conventional niosomes. Both conventional niosomes and pH-sensitive niosomes showed good physicochemical properties at 25°C for 90 days and 40°C for 30 days. Overall, these results suggested that pH-sensitive niosomes may be promoted and used as drug delivery carriers of oryzanol and rice bran oil. Nevertheless, the possible mechanisms of this nanovesicle

formulation need to be investigated in further studies. Ethanol is an alternative to organic solvents (chloroform and methanol) in further studies.

ACKNOWLEDGMENTS

The authors gratefully acknowledge the National Research Council of Thailand (NRCT): N42A650551, the Office of the Higher Education Commission and the Thailand Research Fund (Grant no. RGNS 64–237) for financial support. Grateful thanks also go to Faculty of Pharmaceutical Sciences, Ubon Ratchathani, Thailand for supporting facilities and equipment. In addition, the authors would like to thank the Queen Saovabha Memorial Institute, Thai Red Cross Society, Bangkok, Thailand for kindly providing the shed snake skin used in the pre-formulation study. The authors also cannot forget a special thanks to the LIPOID GmbH (Cologne, Germany) for support in obtaining chemicals.

AUTHOR CONTRIBUTIONS

Sureewan Duangjit contributed to the conceptualization, original draft preparation, performed the statistical analysis and data visualization, wrote the manuscript and supported the funding acquisition. Chudanut Akarachinwanit assisted in conducting the experiments. Warisada Sila-on assisted in the methodology, statistical analysis, data visualization and edited the manuscript. Sureewan Bumrungthai assisted in the methodology, conducting the experiments, statistical analysis, data visualization and edited the manuscript. Praneet Opanasopit supported the funding acquisition. Tanasait Ngawhirunpat assisted in conceptualization.

CONFLICT OF INTEREST

The authors declare no conflicts of interest.

REFERENCES

Abd-Elal R.M., Shamma R.N., Rashed H.M., and Bendas E.R. 2016. Trans-nasal zolmitriptan novasomes: *In-vitro* preparation, optimization and *in-vivo* evaluation of brain targeting efficiency. Drug Delivery. 23: 3374-3386.

Abd E., Roberts M.S., and Grice J.E. 2016. A comparison of the penetration and permeation of caffeine into and through human epidermis after application in various vesicle formulations. Skin Pharmacology and Physiology. 29: 24-30.

Abdelkader H., Alani A.W., and Alany R.G. 2014. Recent advances in non-ionic surfactant vesicles (niosomes): Self-assembly, fabrication, characterization, drug delivery applications and limitations. Drug Delivery. 21: 87-100.

Abri Aghdam M., Bagheri R., Mosafer J., Baradaran B., Hashemzaei M., Baghbanzadeh A., de la Guardia M., et al. 2019. Recent advances on thermosensitive and pH-sensitive liposomes employed in controlled release. Journal of Controlled Release. 315: 1-22

Akarachinwanit C., Sila-on W., Bumrungthai S., Miyazato K., Hayakawa Y., and Duangjit S. 2017. 'Development of rice bran oil load niosomes for anti-aging cosmetics: Comparative study of two preparation methods'. The 7th International Graduate Research Conference (IGR 7)(pp. 101-107). Ubon Ratchathani, Thailand, 19-20 October.

Akbarzadeh A., Rezaei-Sadabady R., Davaran S., Joo S.W., Zarghami N., Hanifehpour Y., Samiei M., et al. 2013. Liposome: Classification, preparation, and applications. Nanoscale Research Letters. 8: 102.

Al Mahrouqi D., Vinogradov J., and Jackson M.D. 2016. Temperature dependence of the zeta potential in intact natural carbonates. Geophysical Research Letters. 43: 511-587.

Bernardi D.S., Pereira T.A., Maciel N.R., Bortoloto J., Viera G.S., Oliveira G.C., and Rocha-Filho P.A. 2011. Formation and stability of oil-in-water nanoemulsions containing rice bran oil: *In vitro* and *in vivo* assessments. Journal of Nanobiotechnology. 9: 44.

Chen S., Hanning S., Falconer J., Locke M., and Wen J. 2019. Recent advances in non-ionic surfactant vesicles (niosomes): Fabrication, characterization, pharmaceutical and cosmetic applications. European Journal of Pharmaceutics and Biopharmaceutics. 144: 18-39.

Cho J.-Y., Lee H.J., Kim G.A., Kim G.D., Lee Y.S., Shin S.C., Park K.-H., et al. 2012. Quantitative analyses of individual γ-oryzanol (*steryl ferulates*) in conventional and organic brown rice (*Oryza sativa* L.). Journal of Cereal Science. 55: 337-343.

Chu C.-J., and Szoka F.C. 1994. pH-sensitive liposomes. Journal of Liposome Research. 4: 361-395.

Danaei M., Dehghankhold M., Ataei S., Hasanzadeh Davarani F., Javanmard R., Dokhani A., Khorasani S., et al. 2018. Impact of particle size and polydispersity index on the clinical applications of lipidic nanocarrier systems. Pharmaceutics. 10: 57.

Duangjit S., Inta T., Ruangkarnjanapaisarn P., and Rungseevijitprapa W. 2016. Effect of cholesterol and oleic Acid on physicochemical properties and stability of liposomes. Isan Journal of Pharmaceutical Sciences. 11: 1-13.

Eid R.K., Essa E.A., and El Maghraby G.M. 2019. Essential oils in niosomes for enhanced transdermal delivery of felodipine. Pharmaceutical Development and Technology. 24: 157-165.

El Maghraby G.M., Barry B.W., and Williams A.C. 2008. Liposomes and skin: From drug delivery to model membranes. European Journal of Pharmaceutical Sciences. 34: 203-222.

Fan Y., Chen C., Huang Y., Zhang F., and Lin G. 2017. Study of the pH-sensitive mechanism of tumor-targeting liposomes, Colloids and surfaces. B, Biointerfaces. 151: 19-25.

Gillet A., Compère P., Lecomte F., Hubert P., Ducat E., Evrard B., and Piel G. 2011. Liposome surface charge influence on skin penetration behavior. International Journal of Pharmaceutics. 411: 223-231.

Guo H.X., Heinämäki J., and Yliruusi J. 2008. Stable aqueous film coating dispersion of zein. Journal of Colloid and Interface Science. 322: 478-484.

Hoeller S., Sperger A., and Valenta C. 2009. Lecithin based nanoemulsions: A comparative study of the influence of non-ionic surfactants and the cationic phytosphingosine on physicochemical behaviour and skin permeation. International Journal of Pharmaceutics. 370: 181-186.

Junyaprasert V.B., Teeranachaideekul V., and Supaperm T. 2008. Effect of charged and non-ionic membrane additives on physicochemical properties and stability of niosomes, AAPS PharmSciTech, 9: 851-859.

Khan D.H., Bashir S., Khan M.I., Figueiredo P., Santos H.A., and Peltonen L. 2020. Formulation optimization and *in vitro* characterization of rifampicin and ceftriaxone dual drug loaded niosomes with high energy probe sonication technique. Journal of Drug Delivery Science and Technology. 58: 101763.

Khoee S., and Yaghoobian M. 2017. Chapter 6 - Niosomes: A novel approach in modern drug delivery systems. In E. Andronescu and A.M. Grumezescu (Eds.), Nanostructures for Drug Delivery (pp. 207-237). Elsevier. Amsterdam.

Khurana S., Jain N.K., and Bedi P.M. 2013. Development and characterization of a novel controlled release drug delivery system based on nanostructured lipid carriers gel for meloxicam. Life Sciences. 93: 763-772.

Kurniawan J., Suga K., and Kuhl T.L. 2017. Interaction forces and membrane charge tunability: Oleic acid containing membranes in different pH conditions. Biochimica et Biophysica Acta. 1859: 211-217.

Lambers H., Piessens S., Bloem A., Pronk H., and Finkel P. 2006. Natural skin surface pH is on average below 5, which is beneficial for its resident flora. International Journal of Cosmetic Science. 28: 359-370.

Leekumjorn S., Cho H.J., Wu Y., Wright N.T., Sum A.K., and Chan C. 2009. The role of fatty acid unsaturation in minimizing biophysical changes on the structure and local effects of bilayer membranes. Biochimica et Biophysica Acta. 1788: 1508-1516.

Manosroi A., Chutoprapat R., Abe M., and Manosroi J. 2008. Characteristics of niosomes prepared by supercritical carbon dioxide ($scCO_2$) fluid. International Journal of Pharmaceutics. 352: 248-255.

Manosroi A., Chutoprapat R., Abe M., Manosroi W., and Manosroi J. 2012a. Anti-aging efficacy of topical formulations containing niosomes entrapped with rice bran bioactive compounds. Pharmaceutical Biology. 50: 208-224.

Manosroi A., Chutoprapat R., Abe M., Manosroi W., and Manosroi. 2012b. Transdermal absorption enhancement of rice bran bioactive compounds entrapped in niosomes. AAPS PharmSciTech. 13: 323-335.

Masarudin M.J., Cutts S.M., Evison B.J., Phillips D.R., and Pigram P.J. 2015. Factors determining the stability, size distribution, and cellular accumulation of small, monodisperse chitosan nanoparticles as candidate vectors for anticancer drug delivery: Application to the passive encapsulation of [(14)C]-doxorubicin, Nanotechnology. Science and Applications. 8: 67-80.

Mertins O., Mathews P.D., and Angelova A. 2020. Advances in the design of pH-Sensitive cubosome liquid crystalline nanocarriers for drug delivery applications. Nanomaterials (Basel). 10: 963.

Mutlu-Agardan N.B., Yilmaz S., Kaynak Onurdag F., and Celebi N. 2021. Development of effective AmB/AmB–αCD complex double loaded liposomes using a factorial design for systemic fungal infection treatment. Journal of Liposome Research. 31: 177-188.

Notman R., Noro M.G., and Anwar J. 2007. Interaction of oleic acid with dipalmitoylphosphatidylcholine (DPPC) bilayers simulated by molecular dynamics. Journal of Physical Chemistry B. 111: 12748-12755.

Patzelt A., Mak W.C., Jung S., Knorr F., Meinke M.C., Richter H., Rühl E., et al. 2017. Do nanoparticles have a future in dermal drug delivery?. Journal of Controlled Release. 246: 174-182.

Peralta M.F., Guzmán M.L., Pérez A.P., Apezteguia G.A., Fórmica M.L., Romero E.L., Olivera M.E., et al. 2018. Liposomes can both enhance or reduce drugs penetration through the skin. Scientific Reports. 8: 13253.

Pinilla C.M.B., Thys R.C.S., and Brandelli A. 2019. Antifungal properties of phosphatidylcholine-oleic acid liposomes encapsulating garlic against environmental fungal in wheat bread. International Journal of Food Microbiology. 293: 72-78.

Rinaldi F., Forte J., Pontecorvi G., Hanieh P.N., Carè A., Bellenghi M., Tirelli V., et al. 2022. pH-responsive oleic acid based nanocarriers: Melanoma treatment strategies. International Journal of Pharmaceutics. 613: 121391.

Rodsuwan U., Pithanthanakul U., Thisayakorn K., Uttapap D., Boonpisuttinant K., Vatanyoopaisarn S., Thumthanaruk B., et al. 2020. Preparation and characterization of gamma oryzanol loaded zein nanoparticles and its improved stability. Food Science & Nutrition. 9(2): 616-624.

Tokudome Y., Nakamura K., Itaya Y., and Hashimoto F. 2015. Enhancement of skin penetration of hydrophilic and lipophilic compounds by pH-sensitive liposomes. Journal of Pharmaceutical Sciences. 18: 249-257.

Seetapan N., Bejrapha P., Srinuanchai W., and Ruktanonchai U.R. 2010. Rheological and morphological characterizations on physical stability of gamma-oryzanol-loaded solid lipid nanoparticles (SLNs). Micron. 41: 51-58.

Soliman M.S., Abd-Allah F.I., Hussain T., Saeed N.M., and El-Sawy H.S. 2018. Date seed oil loaded niosomes: Development, optimization and anti-inflammatory effect evaluation on rats. Drug Development and Industrial Pharmacy. 44: 1185-1197.

Srisuk P., Thongnopnua P., Raktanonchai U., and Kanokpanont S. 2012. Physico-chemical characteristics of methotrexate-entrapped oleic acid-containing deformable liposomes for *in vitro* transepidermal delivery targeting psoriasis treatment. International Journal of Pharmaceutics. 427: 426-434.

Subongkot T., Ngawhirunpat T., and Opanasopit P. 2021. Development of ultradeformable liposomes with fatty acids for enhanced dermal rosmarinic acid delivery. Pharmaceutics. 13(3): 404.

Venditti R. 2008. Temperature effects on the zeta potential. In D. Li (Eds.). Encyclopedia of Microfluidics and Nanofluidics (pp. 1980–1987). Springer, Boston.

Villar M.A.L., Vidallon M.L.P., and Rodriguez E.B. 2022. Nanostructured lipid carrier for bioactive rice bran gamma-oryzanol. Food Bioscience. 50: 102064.

Viriyaroj A., Ngawhirunpat T., Sukma M., Akkaramongkolporn P., Ruktanonchai U., and Opanasopit P. 2009. Physicochemical properties and antioxidant activity of gamma-oryzanol-loaded liposome formulations for topical use. Pharmaceutical Development and Technology. 14: 665-671.

Vonarbourg A., Passirani C., Desigaux L., Allard E., Saulnier P., Lambert O., Benoit J.P., et al. 2009. The encapsulation of DNA molecules within biomimetic lipid nanocapsules. Biomaterials. 30: 3197-3204.

Wonglertnirant N., Ngawhirunpat T., and Kumpugdee-Vollrath M. 2012. Evaluation of the mechanism of skin enhancing surfactants on the biomembrane of shed snake skin. Biological and Pharmaceutical Bulletin. 35: 523-531.

Wuttikul K., and Boonme P. 2016. Formation of microemulsions for using as cosmeceutical delivery systems: Effects of various components and characteristics of some formulations. Drug Delivery and Translational Research. 6: 254-262.

Xu Y.-Q., Chen W.-R., Tsosie J.K., Xie X., Li P., Wan J.-B., He C.-W., et al. 2016. Niosome encapsulation of curcumin: Characterization and cytotoxic effect on ovarian cancer cells. Journal of Nanomaterials. 2016: 6365295.

Yoshie A., Kanda A., Nakamura T., Igusa H., and Hara S. 2009. Comparison of gamma oryzanol contents in crude rice bran oils from different sources by various determination methods. Journal of Oleo Science. 58: 511-518.

Yu Y.-Q., Yang X., Wu X.-F., and Fan Y.-B. 2021. Enhancing permeation of drug molecules across the skin via delivery in nanocarriers: Novel strategies for effective transdermal applications. Frontiers in Bioengineering and Biotechnology. 9: 646554.

Zakir F., Vaidya B., Goyal A.K., Malik B., and Vyas S.P. 2010. Development and characterization of oleic acid vesicles for the topical delivery of fluconazole. Drug Delivery. 17: 238-248.

OPEN access freely available online
Natural and Life Sciences Communications
Chiang Mai University, Thailand. https://cmuj.cmu.ac.th